Universität Basel
Departement Umweltwissenschaften

mcr meteorology climatology remote sensing

ICAM 2015 Innsbruck Austria
Poster Session 2 | P2.39

Visualization of high-resolution surface temperature data collected in the Barringer Meteor Crater during METCRAX II

I. Feigenwinter[1], R. Vogt[1], M. Müller[1], E. Parlow[1], M. Grudzielanek[2], M. Maric[2], C. D. Whiteman[3], M. Lehner[3], S. W. Hoch[3]

[1] University of Basel, Department of Environmental Sciences, Meteorology, Climatology and Remote Sensing (MCR), Basel, Switzerland

[2] Ruhr-University of Bochum (RUB), Geographic Institute, Climatology Group, Bochum, Germany

[3] University of Utah, Department of Atmospheric Sciences, Mountain Meteorology Group, Salt Lake City, Utah

INTRODUCTION

Thermal remote sensing is a widely used tool, for both macro-scale observations from satellite-based platforms and micro-scale observations from ground-based infrared cameras. It is often used in urban environments (Voogt and Oke, 2003) and also for sensing tree surface temperatures (Leuzinger et al., 2009, Meier and Scherer, 2012).
During intensive operational periods (IOPs) of the Second Meteor Crater Experiment (METCRAX II) three infrared (IR) cameras recorded high-resolution (0.5 Hz) brightness temperatures - here referred to as surface temperatures (STs) - of the crater. We present a method to project the 2D IR images onto a digital elevation model (DEM) to obtain georeferenced pixels. The bird's eye view helps to qualitatively analyze the fluctuations in ST that are linked to the airflow and the downslope-windstorm-type flows (DWFs), the main phenomenon of interest in METCRAX II.

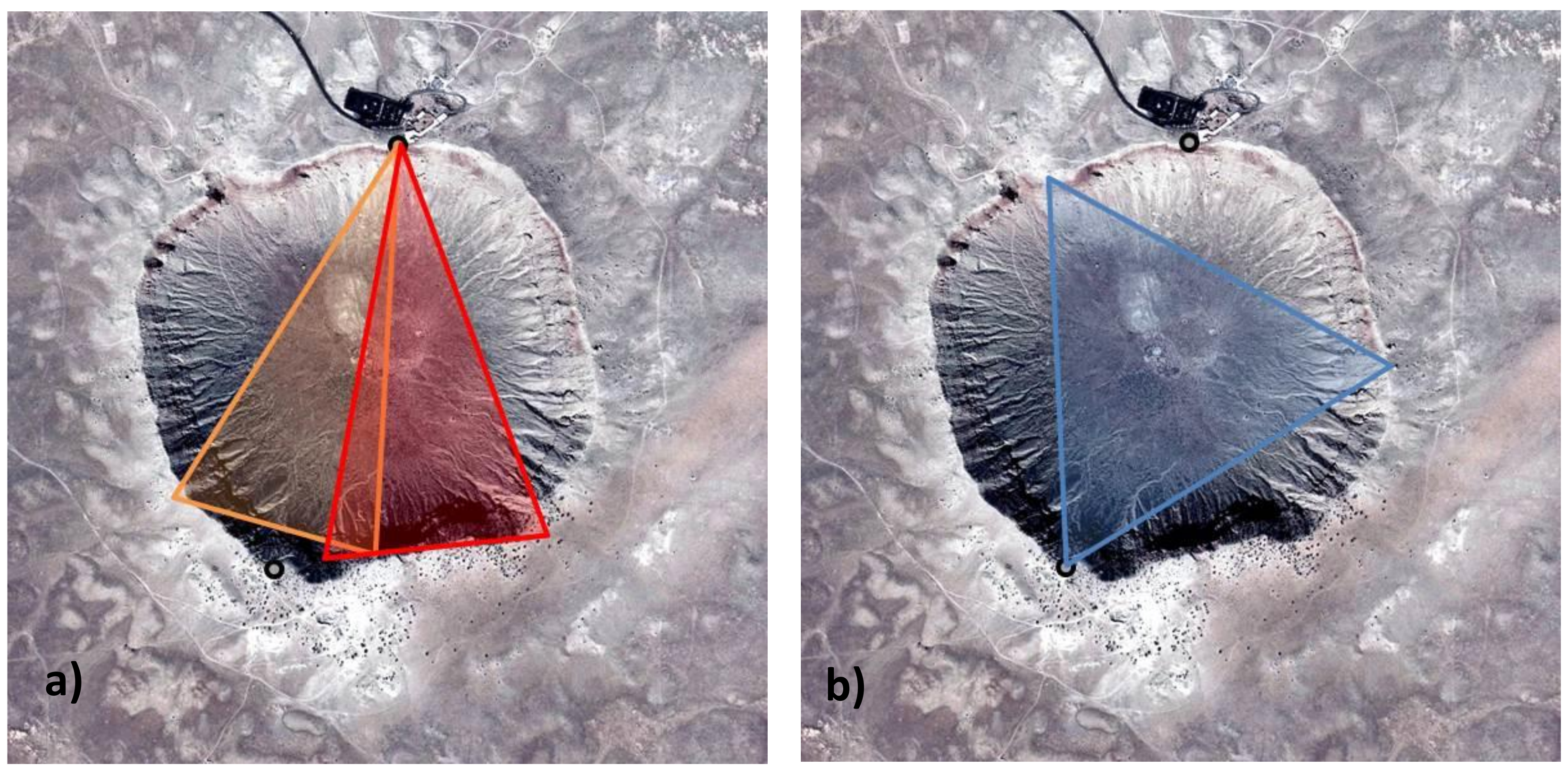

Fig. 1: Schematic orientation of the three cameras from a) north rim to south and b) south rim to north. Orthophoto from USGS

METHODS

Two VarioCAM® hr research 600 time-lapse IR cameras (Infratec, Dresden) were installed on the north rim (here called IRPD and IRDD) and one VarioCAM® HD research 800 camera (IRHD) was installed on the south rim, with all cameras pointing into the crater (Fig. 1). Table 1 lists the characteristics of the three cameras.

Tab. 1: Position of IR cameras and their specification

Name	Lat [°N]	Long [°E]	Resolution [Pixels]	Field of View [°]	Lens
IRPD/IRDD	35.03243	-111.02179	640 x 480	30 x 23	Normal
IRHD	35.02242	-111.02545	1024 x 768	60.3 x 47	Wide angle

The field of view (FOV) of the cameras was used to construct virtual lines of sight (Fig. 2) to identify intersections between pixels and the DEM. For each pixel a horizontal and a vertical angle were calculated. A linear lens function was used for the hr cameras and an empirically adjusted square function was used for the HD camera. The absolute camera orientations (tilt and view angle) were determined using an iterative approach. An interpolation for the missing points in between was made by averaging the surrounding georeferenced pixels.

For better visualization of the airflow, the spatiotemporal fluctuations were calculated using:

$$T_f = T_s - \overline{T}_s" - \langle T_s \rangle' - \langle \overline{T}_s \rangle$$

(Vogt, 2008) where T_s is the original time series of the IR images with the dimensions [640,480,900] for IRDD/IRPD, $\overline{T}_s$" is the picture of the deviations of the temporally averaged picture from the total average [640,480], $\langle T_s \rangle'$ is the time series of deviations of the picture averages from the total average [900] and $\langle \overline{T}_s \rangle$ is the total average [1]. The result is the spatiotemporal variation T_f .

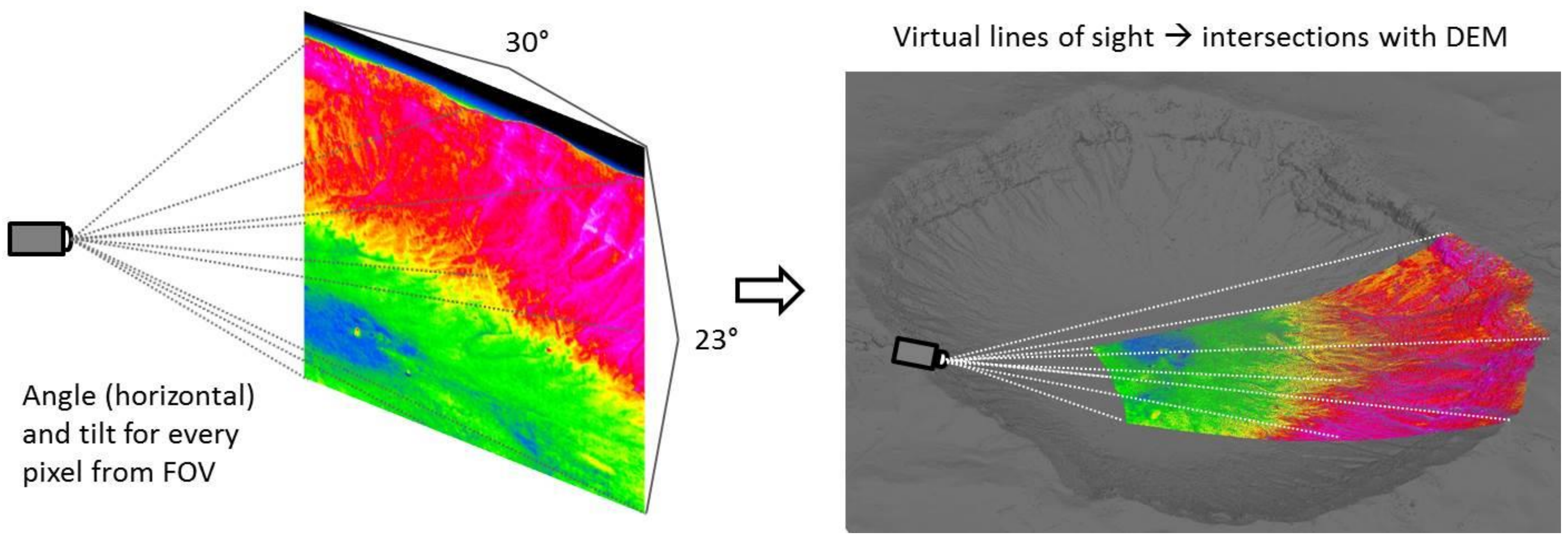

Fig. 2: Scheme of projecting the 2D IR image onto the 3D DEM using the field of view of the image and virtual lines of sight

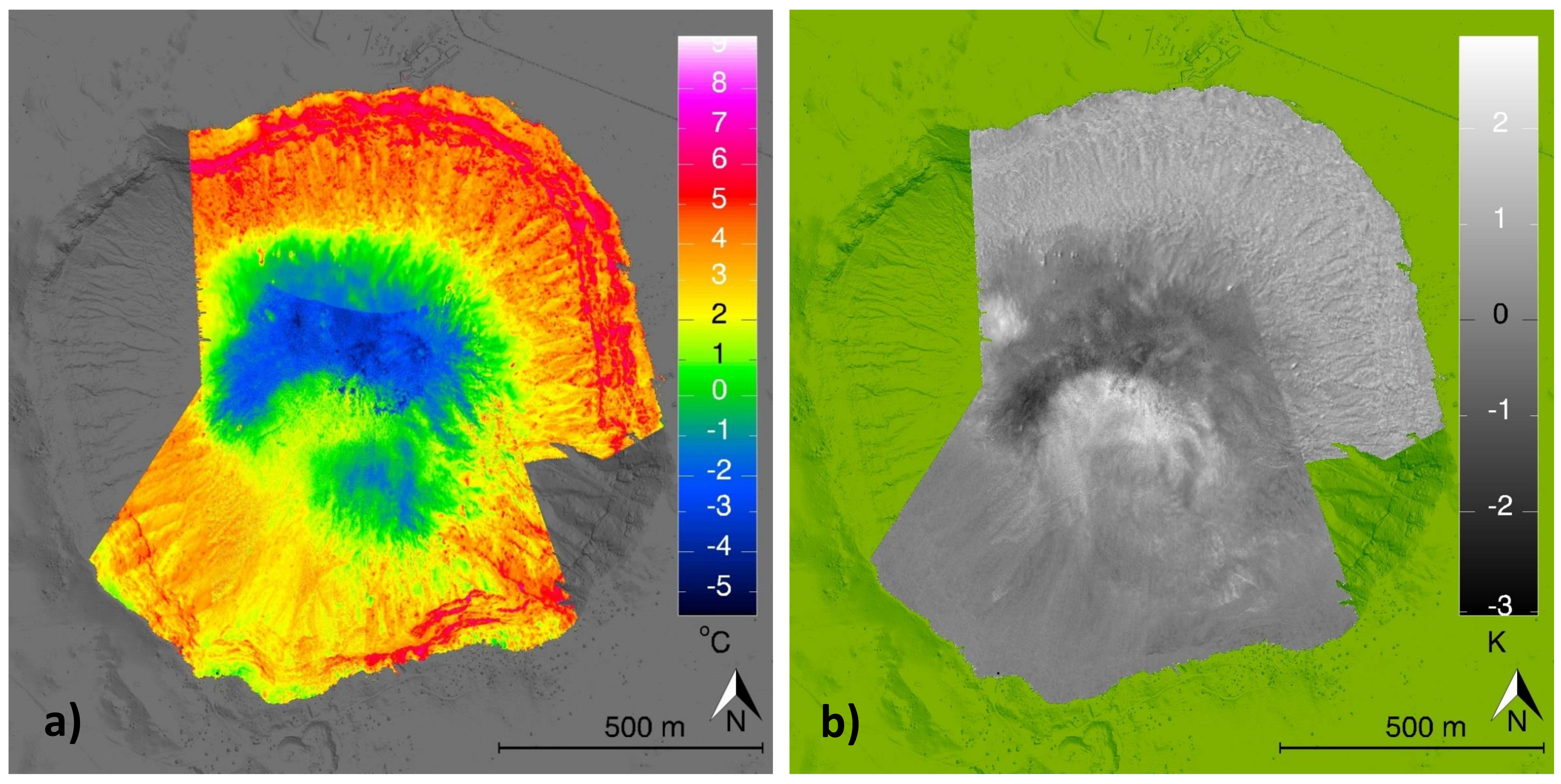

Fig. 3: a) Absolute STs of the crater at 10-19-2013 22:41:32 MST and b) spatiotemporal temperature fluctuations

RESULTS

Projected IR images provide a synopsis of STs and visualize the spatial distribution of temperature inversions that develop in the crater during clear and undisturbed nights (Fig. 3a)(Adler et al., 2012). The absolute STs in Fig. 3a reflect the shallow cold air pool that forms on the crater floor. The surrounding crater walls are up to 10 °C warmer. Higher STs propagate from the southwestern crater rim into the crater. This is probably linked to warmer air intruding from above due to the investigated DWFs . The intruding flow results in temperature fluctuations of up to 2 K as shown in Fig. 3b.

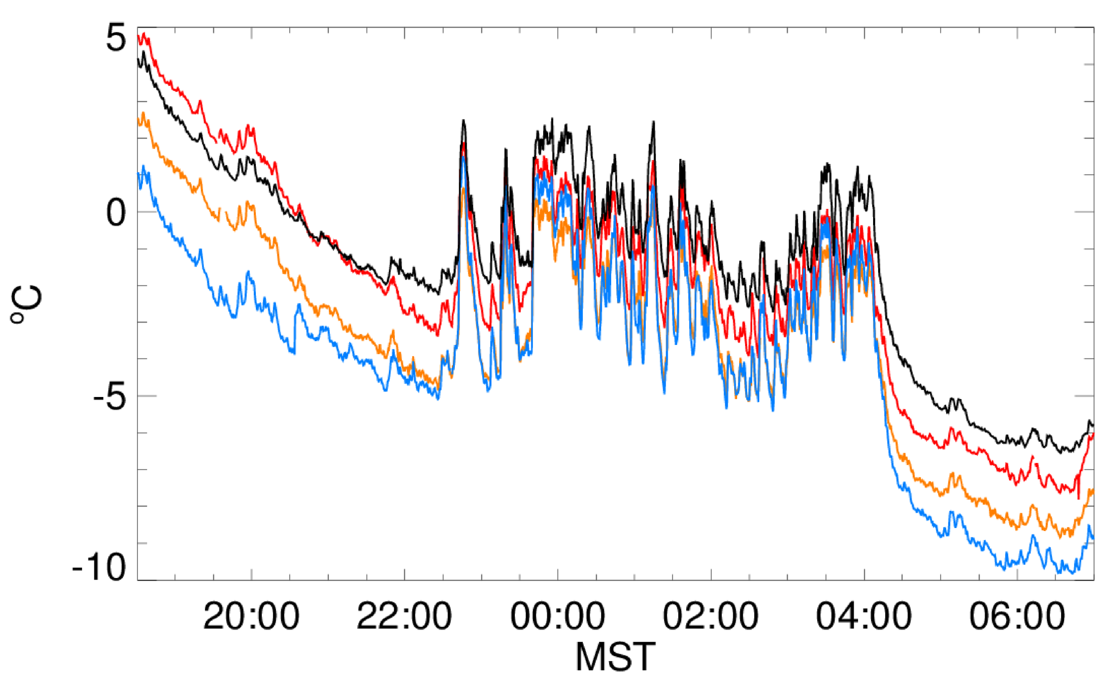

Fig. 4: ST derived from pyrgeometer (black), IRDD (orange), IRPD (red) and IRHD (blue) during IOP4

The georeferencing allowed us to compare the STs derived from the IR cameras during IOP4 with data from a research quality pyrano-meter installed on the crater floor (Fig. 4). STs from the three cameras differed substantially, probably mainly due to differing camera properties and partially due to the fact that no atmospheric corrections were applied. STs decreased after sunset due to radiative cooling. The period between 22:30 and 04:00 is dominated by warm air intrusions (WAI, s. Adler et al., 2012) that lead to increased wind speed and turbulence.

CONCLUSION

High-resolution infrared thermography allows a qualitative analysis of air flow provided that the surface reacts fast enough to changes in air temperature. Various flow structures can be identified using the spatiotemporal temperature fluctuations. The georeferencing of IR images supplies further prospects of research. For example, comparisons can be made with other instruments, and volume calculations can be made for the cold air pool in the crater.

ACKNOWLEDGEMENT

Cameras were provided by Infratec (M.G. Kraus), C. Bernhofer (TU Dresden) and A. Pitacco (U. Padova)
The METCRAX II research was supported by National Science Foundation grants AGS-1160730 and AGS-1160737 and by International Bureau of BMBF grant 01 DM 13002
The University of Basel contributed travel funds

REFERENCES

Adler, B., Whiteman, C.D., Hoch, S.W., Lehner, M. and Kalthoff N.(2012): Warm-Air Intrusions in Arizona's Meteor Crater. *J Appl Meteorol 51*: 1010-1025

Leuzinger, S., Vogt, R. and Körner, C. (2009): Tree surface temperature in an urban environment. *Agric For Meteorol 150*: 56–62

Meier, F. and Scherer, D. (2012): Spatial and temporal variability of urban tree canopy temperature during summer 2010 in Berlin, Germany. *Theor Appl Climatol 110*: 373-384, Springer

Vogt, R. (2008), Visualisation of turbulent exchange using a thermal camera, Paper no. 8B.1, 18th symposium on boundary layer and turbulence, Stockholm.

Voogt, J.A., and Oke ,T.R. (2003): Thermal remote sensing of urban climates. *Remote Sensing of Environment 86:* 370-384

RESPONSIBLE AUTHOR'S ADDRESS

Iris Feigenwinter
MCR-Lab, University of Basel
Klingelbergstrasse 27
CH-4056 Basel
E-mail: iris.feigenwinter@unibas.ch
Tel: +41 61 267 07 49